ACS APPLIED MATERIALS & INTERFACES

Research Article

www.acsami.org

Soluble and Meltable Hyperbranched Polyborosilazanes toward High-Temperature Stable SiBCN Ceramics

Jie Kong,*[,†] Minjun Wang,[†] Jianhua Zou,[‡] and Linan An*[,‡]

[†]MOE Key Laboratory of Space Applied Physics and Chemistry, Shaanxi Key Laboratory of Macromolecular Science and Technology, School of Science, Northwestern Polytechnical University, Xi'an, 710072, P. R. China

[‡]Department of Materials Science and Engineering, Advanced Materials Processing and Analysis Center, University of Central Florida, Orlando, Florida 32816, United States

Supporting Information

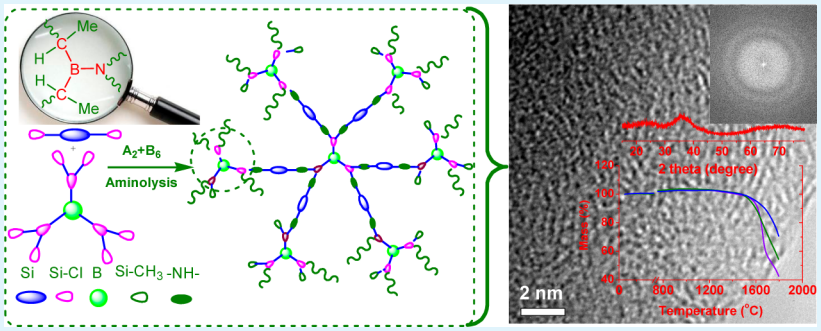

ABSTRACT: High-temperature stable siliconborocarbonitride (SiBCN) ceramics produced from single-source preceramic polymers have received increased attention in the last two decades. In this contribution, soluble and meltable polyborosilazanes with hyperbranched topology (hb-PBSZ) were synthesized via a convenient solvent-free, catalyst-free and one-pot A_2 + B_6 strategy, an aminolysis reaction of the A_2 monomer of dichloromethylsilane and the B_6 monomer of tris-(dichloromethylsilylethyl)borane in the presence of hexamethyldisilazane. The amine transition reaction between the intermediates of dichlorotetramethyldisilazane and tri(trimethylsilylmethylchlorosilylethyl)borane led to the formation of dendritic units of aminedialkylborons rather than trialkylborons. The cross-linked hb-PBSZ precursors exhibited a ceramic yield higher 80%. The resultant SiBCN ceramics with a boron atomic composition of 6.0−8.5% and a representative formula of $Si_1B_{0.19}C_{1.21}N_{0.39}O_{0.08}$ showed high-temperature stability and retained their amorphous structure up to 1600 °C. These hyperbranched polyborosilazanes with soluble and meltable characteristics provide a new perspective for the design of preceramic polymers possessing advantages for high-temperature stable polymer-derived ceramics with complex structures/shapes.

KEYWORDS: *hyperbranched, polyborosilazanes, soluble polymeric precursors, SiBCN ceramics, high-temperature stability*

INTRODUCTION

Polymer-derived ceramics (PDCs) are a class of multifunctional ceramics synthesized by thermal decomposition of preceramic polymers, which possess advantages over conventional polycrystalline ceramics.[1−3] By using a controlled pyrolysis of preceramic polymers or oligomers containing silicon, nitrogen, carbon and boron, quaternary siliconborocarbonitride (SiBCN) ceramics with predefined composition and structure can be produced. Since the pioneering work of Riedel et al. was published in 1996,[4] quaternary SiBCN ceramics have received increasing attention due to their exceptional high-temperature stability,[5−7] creep resistance,[8] tunable semiconducting behavior and significant piezoresistivity even at ultrahigh temperatures.[9,10] They are considered as materials for high-temperature microsensors,[11,12] microelectronic devices,[13] membranes,[14] and high-temperature stable ceramic fibers.[15,16]

In the SiBCN or SiBC system, boron plays a key role in the formation of the amorphous structure, retards the decomposition of silicon-nitride bonds and reduces the diffusion of different species involved in the carbothermal reaction at high temperatures.[4,17] The macromolecular design and synthesis of boron-containing preceramic polymers allow the possibility to tailor their elemental composition and macromolecular hierarchical structures, which in turn determines and optimizes the properties of SiBCN ceramics. Various approaches have been employed to synthesize boron-containing preceramic polymers, mainly including (i) the aminolysis of boron-containing monomers possessing B−Cl, B−Br, or Si−Cl bonds in the presence of ammonia or hexamethyldisilazane (HMDS),[18] (ii) a dehydrogenative coupling reaction of preceramic polymers with borane derivatives,[19,20] and (iii) the hydroboration of unsaturated groups on preceramic polymers

Received: January 8, 2015
Accepted: March 16, 2015
Published: March 16, 2015

DOI: 10.1021/am509129a
ACS Appl. Mater. Interfaces 2015, 7, 6733−6744

with monofunctional, difunctional or multifunctional boranes.[21,22] These boranes mainly contain monofunctional 9-borabicyclo[3,3,1]nonane (9-BBN) or pinacolborane, difunctional substituted boranes of H_2BR (R = organic residue or halogen atom), and multifunctional B_2H_6, BH_3·donors, and borazine. For example, ceramic membranes were prepared from highly processable polyborosilazanes obtained via the hydroboration of cyclic silazanes by lowering the reaction temperature.[23] If the hydroboration of cyclic silazanes is kept for long, the polymer solution will become gelation, although there is a time window for the processing of the polyorganoborosilazane solution, for example, by the dip-coating of an alumina substrate inside it.[23]

Normally, both the aminolysis polymerization of boron-containing monomers such as dimethyl etherate trichloroborine and the hydroboration modification of polysilazane with multifunctional BH_3· donors are not easily controlled, usually yielding insoluble cross-linked polyborosilazanes.[24−26] With respect to potential applications as ceramic precursors, solubility is useful for further processing because the precursors often need to form complex shapes before they are cross-linked, pyrolyzed and converted to SiBCN ceramics. In comparison to their linear counterparts, boron-containing preceramic polymers with hyperbranched topology offer the following advantages: (i) higher solubility and lower viscosity due to their compact conformation and decreased interchain entanglements,[27−31] (ii) the boron in multifunctional boranes can be conveniently introduced into the soluble polymers by the so-called $A_2 + B_n$ ($n \geq 3$) approach,[32−36] and (iii) the hyperbranched topology may benefit the homogeneous distribution of boron on an atomic scale in either preceramic polymers or pyrolyzed ceramics.[37] Thus, fine regulation of the polymerization is needed to achieve soluble hyperbranched polymers with a high molecular weight.

For the synthesis of hyperbranched polymers, P. J. Flory think that only low molar mass products are obtained because gelation occurs at very low monomer conversions based on two assumptions: the reactivity of the functional groups remains constant during polymerization and the reactions do not involve cyclization.[38] Actually, the first condensation reaction of A_2 and B_3 monomer is faster than the subsequent propagation[39] and various cyclic species can be identified using matrix assisted laser desorption ionization/time-of-flight mass spectrometry (MALDI-TOF-MS) analysis,[40] both of which shift the gel point to higher conversions. If the polymerization process is regulated, the polymers with hyperbranched topology and high molecular weight can be achieved.[41]

In this contribution, a facile solvent-free, catalyst-free and one-pot strategy was developed to synthesize hyperbranched polyborosilazanes (hb-PBSZ) based on the aminolysis reaction of A_2 monomers of dichloromethylsilane (DCMS) with B_6 monomers of tris(dichloromethylsilylethyl)borane (TDSB) in the presence of HMDS. The dendritic units in the resulting hb-PBSZ were identified to be amine-boranes, i.e., aminedialkylborons, rather than trialkylborons, because of the amine transition reaction. The meltable hb-PBSZ show good solubility in aliphatic and aromatic solvents such as THF, $CDCl_3$ and toluene. To the best of our knowledge, soluble and meltable hyperbranched polyborosilazanes have not been reported yet. When hb-PBSZ with high ceramic yield were pyrolyzed at a high temperature, quaternary SiBCN ceramics with a uniform boron dispersion were obtained, which were amorphous even after being annealed at a high temperature.

EXPERIMENTAL SECTION

Materials. Borane dimethylsulfide complex (2.0 M in tetrahydrofuran), dichloromethylvinylsilane (DCMVS), dichloromethylsilane (DCMS), hexamethyldisilazane (HMDZ), and 4-methoxyphenol were purchased from Alfa Aesar China and used as received. Anhydrous tetrahydrofuran (THF) was freshly distilled for use under reflux using sodium/benzophenone.

Synthesis of Tris(dichloromethylsilylethyl)borane (TDSB). Under an argon atmosphere, a 100 mL flame-dried flask equipped with a Teflon stir bar, septum, and high-vacuum stopcock was charged with DCMVS (5.16 g, 35.5 mmol) and cooled down to 0 °C in ice/water bath. The borane dimethylsulfide solution (5.9 mL, 11.8 mmol) was added through an argon-purged syringe. The reaction was conducted at ambient temperature for 24 h with stirring under argon. For offline NMR characterization, 0.5 mL solution was taken out using an argon-purged syringe and dried by evaporating solvent through vacuum (35 °C, 0.04 bar) distillation.

Synthesis of Hyperbranched Polyborosilazane with Si−H Bonds. For the synthesis of hyperbranched polyborosilazane with Si−H bonds (hb-PBSZ-SiH), DCMS (1.36 g, 11.8 mmol), HMDZ (15.9 g, 98.8 mmol), and the inhibitor 4-methoxyphenol (10 mg) were added in sequence to the flask containing the TDSB solution at ambient temperature. The reaction was conducted at 110 °C for 24 h under reduced pressure (0.1 bar) to remove the small molecular byproducts of trichloromethylsilane and the residue THF. The reaction was then heated to 180 °C for 2 h under reduced pressure to further the reaction and remove byproducts. Finally, yellow glassy solids were obtained (5.9 g, 65% yield).

Synthesis of Hyperbranched Polyborosilazane with Si−H Bonds and Vinyl Groups. The synthesis procedure of hyperbranched polyborosilazane with Si−H bonds and vinyl groups (hb-PBSZ-SiH-Vi) is similar to hb-PBSZ-SiH. However, the DCMS was substituted by DCMVS. The products of hb-PBSZ-SiH-Vi were also yellow glassy solids with a 60% yield.

Ceramics Conversion. Approximately 2.0 g of as-synthesized hb-PBSZ-SiH or hb-PBSZ-SiH-Vi were transferred into a tube furnace (GSL-1700X, Kejing New Mater. Ltd., China) for pyrolysis under an argon stream. The cross-linking reaction was performed at 200 °C (heating rate: 5 K/min, holding time: 2 h) followed by pyrolysis at 900 °C (heating rate = 5 K/min, holding time = 4 h). Afterward the samples were cooled to ambient temperature. The resulting ceramic materials were milled into powders for further experiments. The annealing of pyrolyzed ceramics at different temperatures was conducted in a tube furnace under a nitrogen stream (heating rate = 3 K/min, holding time = 2 h). For example, the ceramic annealed at 1600 °C was treated at 1100, 1300, 1500, and 1600 °C for 2 h each.

Characterization. Nuclear magnetic resonance (NMR) measurements were carried out on a Bruker Avance 500 spectrometer (Bruker BioSpin, Switzerland) to collect the ^1H, ^{13}C, and ^{11}B spectra. Chemical shifts are referenced to tetramethylsilane (TMS). ^{11}B NMR spectra were obtained on an NMR spectrometer equipped with the appropriate decoupling accessories. The ^{11}B chemical shifts are referenced to BF_3·OEt_2 (0.0 ppm) with a negative sign indicating an upfield shift.

Fourier transform infrared spectroscopy (FT-IR) measurements were conducted on an FT-IR spectrophotometer (PerkinElmer, USA). Raman Spectroscopy studies were performed using a Raman Microprobe Instrument (Invia, Renishaw, USA) with 514.5 nm Ar^+ laser excitation.

Boron elemental analysis of polymers was performed on an inductively coupled plasma-atomic emission spectrometer (IRIS Advantage ER/S, Thermo Fisher Scientific, Waltham, USA). The hb-PBSZs samples were calcinated under 600 °C for 24 h. The chars were then dissolved in 15 mL of a boiling mixture of nitric acid and hydrochloric acid (1:3 v/v). Finally, the solution was diluted to 25 mL with deionized water for determination using a boron standard solution (1.00 mg/mL).

Size exclusion chromatography (SEC) measurements were performed on a system equipped with a Waters 515 pump, an autosampler and two MZ gel columns (10^3 and 10^4 Å) with a flow rate

DOI: 10.1021/am509129a
ACS Appl. Mater. Interfaces 2015, 7, 6733−6744

of 0.5 mL/min in THF (HPLC grade) at 25 °C. The detectors included a differential refractometer (Optilab rEX, Wyatt) and a multiangle light scattering detector (MALS, Wyatt) equipped with a 632.8 nm He−Ne laser (DAWN EOS, Wyatt). The refractive index increments of the polymers in THF were measured at 25 °C using an Optilab rEX differential refractometer.

Thermogravimetric analysis coupled with mass spectrometry was performed using a simultaneous thermoanalyzer STA 449 F3 coupled with a quadrupole mass spectrometer QMS 403 C Aëolos (Netzsch Group, Germany) at temperatures ranging between 40 and 1400 °C with a heating rate of 10 K/min in argon atmosphere (gas flow, 50 mL/min). High-temperature thermogravimetric analysis was conducted on a thermoanalyzer STA 429 CD with a crucible of ZrO_2 (Netzsch Group, Germany) at temperatures ranging between 40 and 1800 °C with a heating rate of 5 K/min in helium atmosphere (gas flow, 50 mL/min).

Imaging X-ray photoelectron spectroscopy (XPS) measurements were conducted on a K-Alpha spectrometer (Axis Ultra, Kratos Analytical Ltd., U.K.) and the core level spectra were measured using a monochromatic Al Kα X-ray source ($h\nu$ = 1486.7 eV). The analyzer was operated at 23.5 eV pass energy and the analyzed area was 200−800 μm in diameter. The lowest energy resolution is 0.48 eV (Ag 3d5/2). Binding energy was referenced to the adventitious hydrocarbon C 1s line at 285.0 eV. The curve fitting of the XPS spectra was performed using the least-squares method.

Elements analysis of ceramics was conducted at the Shanghai Institute of Ceramics, Chinese Academy of Science. The silicon and boron content in the ceramics was determined by inductively coupled plasma atomic emission spectroscopy (ICP-AES, Vista AX, Varian Corporation, U.S.A.). Before the measurement, the ceramics were mixed with sodium hydroxide and melted at high temperature and subsequently dissolved by nitric acid in moderate conditions. The carbon content was determined by the combustion-coulomb method, calculating the amount of electric charge during the neutralization of the solution with unbalanced pH values produced by carbon dioxide from the combustion of sample in oxygen. The nitrogen and oxygen content was analyzed by Oxygen-Azote mensuration equipment (TC600, Leco Co., Ltd., U.S.A.). The measurement grade of each sample was 10 g.

Powder X-ray diffraction (XRD) measurements were conducted on an X'Pert Pro Powder diffractometer from PANalytical (Cu Kα radiation, 40 kV, 40 mA) (PANalytical B.V., Netherlands). The X'Celerator Scientific RTMS detection unit was used for detection.

Transmission electron microscopy (TEM, FEI Tecnai G2 F30) was operated at 200 kV, coupled with electron diffraction analysis. A 5 μL droplet of an ultrasonically dispersed mixture of milled sample and alcohol (0.02 mg/mL) was dropped onto a copper grid (200 mesh) coated with carbon film and dried at ambient temperature for 30 min.

RESULTS AND DISCUSSION

Synthesis of Tris(dichloromethylsilylethyl)borane. The B_6 monomer of TDSB was synthesized via a hydroboration reaction between borane dimethylsulfide complex and DCMVS (Scheme 1).[42] The ^{11}B and ^{13}C NMR spectra of the resulting TDSB are presented in Figure 1. Compared to the starting monomer of DCMVS, the characteristic signals of carbons in the vinyl groups at 131−138 ppm have completely disappeared. At the same time, in Figure 1a, the characteristic signals at 11 and 34 ppm verify the occurrence of the β addition between borane dimethylsulfide complex and DCMVS. The signals between 14−19 ppm indicate the existence of ethylene groups on the TDSB. Additionally, the hydroboration reaction was verified by the obtained ^{11}B NMR spectrum in Figure 1b. The appearance of the new peak at 82.9 ppm is assigned to boron atoms linked to three ethylene groups as depicted in Scheme 1. These boron atoms were derived from the total hydroboration between borane dimethylsulfide complex and DCMVS. In addition to the main peak at 82.9 ppm, two smaller peaks at 50.9 and 29.9 ppm appear, which are respectively attributed to dialkyl borate and alkyl borate produced by the hydrolysis or oxidation of TDSB during storage or measurement. Because the hydrolysis and oxidation of the TDSB occurred even in Schlank flasks under argon protection, we decided to synthesize the hb-PBSZ directly by using the TDSB solution.

Scheme 1. Synthetic Route for Tris(dichloromethylsilylethyl)borane from Borane Dimethylsulfide Complex and Dichloromethylvinylsilane

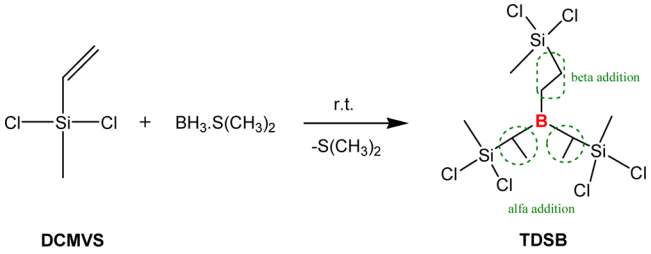

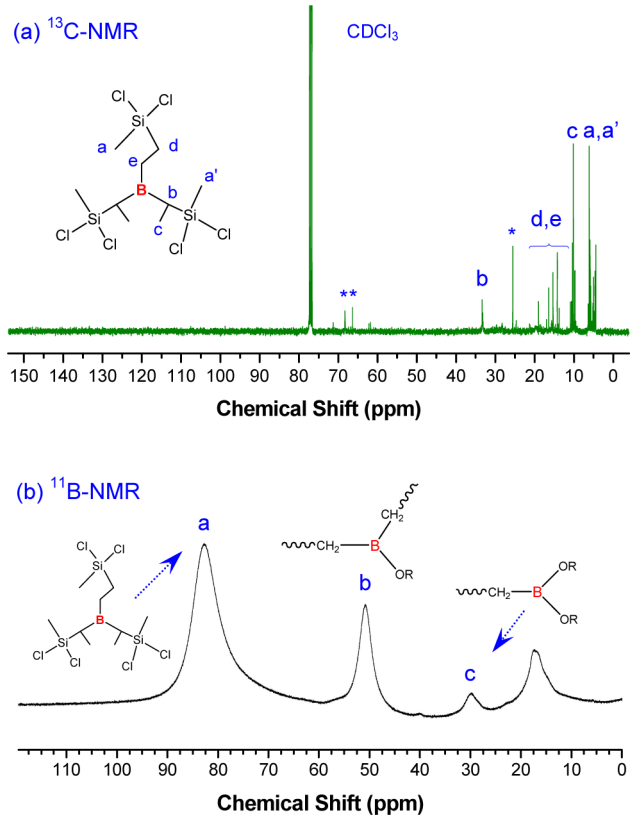

Figure 1. ^{13}C NMR spectrum (a) and ^{11}B NMR spectrum (b) of TDSB dissolved in $CDCl_3$. The stars represent residual THF solvent.

Synthesis of Soluble Hyperbranched Polyborosilazanes. The hyperbranched polyborosilazanes (hb-PBSZ) were synthesized through an aminolysis reaction between TDSB and DCMS (or DCMS and DCMVS) in the presence of an overdose of HMDS. The reaction route is schematically described in Scheme 2. By regulating the feed ratio of the A_2 and B_6 monomers and stopping the reaction before it reaches the gel point, soluble polymers with predefined terminal groups (Si−H or vinyl) can be obtained; hb-PBSZ with Si−H bonds (hb-PBSZ-SiH, P1−P2) or both Si−H bonds and vinyl groups

DOI: 10.1021/am509129a
ACS Appl. Mater. Interfaces 2015, 7, 6733−6744

Scheme 2. Synthetic Route for Soluble Hyperbranched Polyborosilazanes from TDSB, DCMVS, and HMDS at Temperatures from 110 to 180 °C[a]

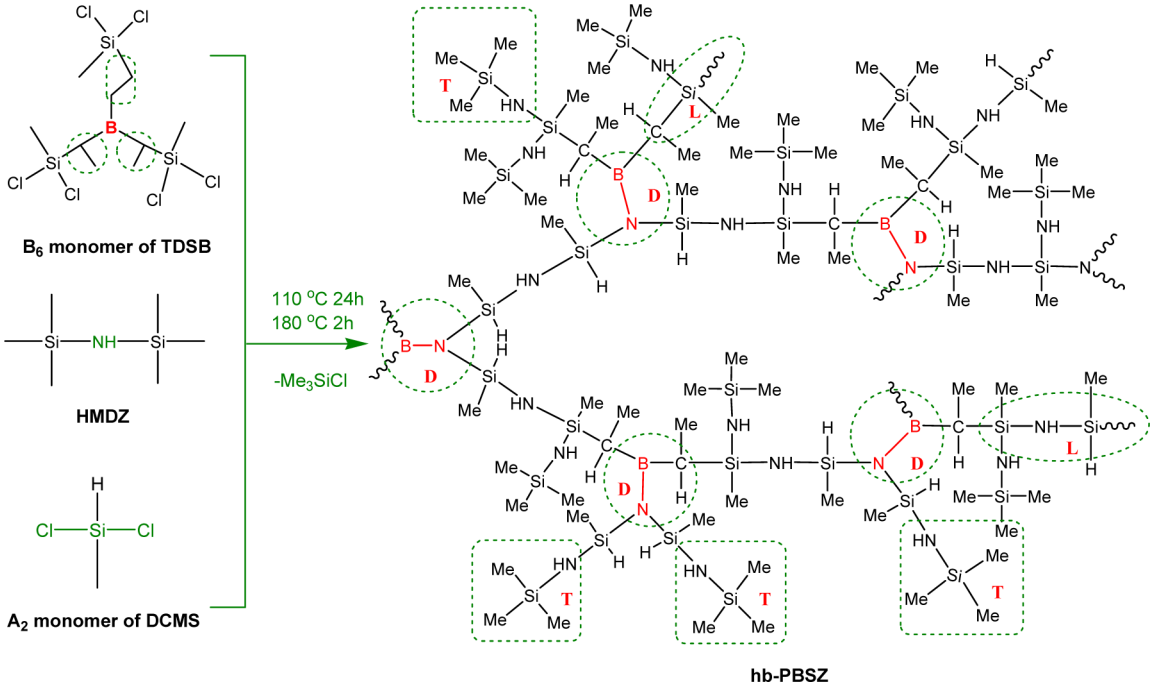

[a]D: Dendritic unit (aminedialkylboron, $(—C_2H_4)_2—B—N═$)). L: Linear unit (disilazane ($—SiRCH_3—NH—SiRCH_3—$)). T: Terminal unit (trimethylsilyl groups ($—NH—Si(CH_3)_3$)).

(hb-PBSZ-SiH-Vi, P3−P4) were synthesized. They are very soluble in aliphatic and aromatic solvents such as THF, DMF, $CDCl_3$ and toluene. In addition, they are meltable at 120−150 °C and fiber-like structures can be easily formed. Good solubility is convenient for subsequent characterization and processing of shaped patterns or bodies and the meltable property is helpful in melt spinning for the formation of SiBCN fibers as shown in Figure S1 (Supporting Information). In general, hydroboration of borane dimethylsulfide and poly- or oligo-silazanes with vinyl groups or direct aminolysis of boron-containing monomers possessing B−Cl bonds always leads to cross-linked or slightly cross-linked polyborosilazanes. Here, the hyperbranched topology design of polyborosilazane via a convenient $A_2 + B_6$ strategy gives a strong possibility to extend the polymeric precursors with soluble and tunable properties.

The ^{1}H NMR spectrum shown in Figure 2a reveals the existence of Si−H bonds with a δ of 4.6−4.8 ppm, vinyl groups with a δ of 5.6−6.2 ppm and ethylene groups with a δ of 0.4−1.7 ppm in the resulting hb-PBSZ-SiH-Vi (P3−P4). On the other hand, only the existence of a Si−H bond with a δ of 4.6−4.9 ppm and an ethylene group with a δ of 0.7−1.7 ppm in the resulting hb-PBSZ-SiH (P1−P2) could be confirmed in Figure 2b. The amines on the silazane units and the Si−H bonds were also confirmed by the peaks at 2110 cm^{-1} in the FTIR spectra in Supporting Information Figure S2 for all the as-synthesized polymers (P1−P4). The obtained hb-PBSZ were characterized by SEC (Figure 3) and shown to possess a number-average molecular weight (M_n) of 2670−7870 g/mol and a polydispersity index (PDI) of 1.5−1.7 (Table 1). The molecular weight M_n is much higher than that of some commercial polysilazanes (700−1200 g/mol).[43] Because of this high molecular weight, the resulting hb-PBSZ are viscous liquids or elastomer-like states of yellow color.

Here, the as-synthesized TDSB in solution was directly employed to synthesize the polymers to avoid atmospheric moisture. In comparison to the TDSB spectrum in Figure 1b, no characteristic signal at 52−54 ppm (assigned to dialkyl borate) was observed in the ^{11}B NMR spectrum (Figure 2c). The signals at 47.85 ppm in Figure 2c clearly indicate that the boron atoms are attached to one nitrogen atom and two ethylene groups.[44] The dendritic units of these soluble hb-PBSZ are therefore aminedialkylborons (a type of amine-boranes) rather than the trialkylboron units obtained after the aminolysis reaction between TDSB and DCMS as presented in Scheme 2.

The proposed formation mechanism for the dendritic units of the hb-PBSZ is shown in Scheme 3. First, when one of the silicon-chloride bonds of TDSB or DCMS is substituted by an amine during aminolysis, the decreased electrophilicity makes the substitution of another silicon-chloride bond more difficult. Thus, the intermediates tri(trimethylsilylmethylchlorosilyl-ethyl) borane (TTMCB) and dichlorotetramethyldisilazane (DCTMSZ) were formed at 110 °C from the aminolysis of TDSB and DCMS, respectively, accompanied by the elimination of trimethylchlorosilane. Second, the trialkylboron in TTMCB will preferably react with the amine in DCTMSZ rather than the amine in HMDS because of steric hindrance to form the amine-borane bond in aminedialkylboron. It is well-known that the amine-borane bond in trialkylboron can be formed in the presence of amine when catalyzed by thiol at 20−100 °C.[45,46] Here, the reaction was conducted at a higher temperature of 110−180 °C without the use of catalysts. The secondary amine group in DCTMSZ is covalently bonded to the boron atom on TTMCB. Subsequently, the nitrogen−hydrogen bond and boron−carbon bond are broken and the hydrogen atoms attached to the ethylene carbons with minimum steric hindrance, resulting in the formation of the

DOI: 10.1021/am509129a
ACS Appl. Mater. Interfaces 2015, 7, 6733−6744

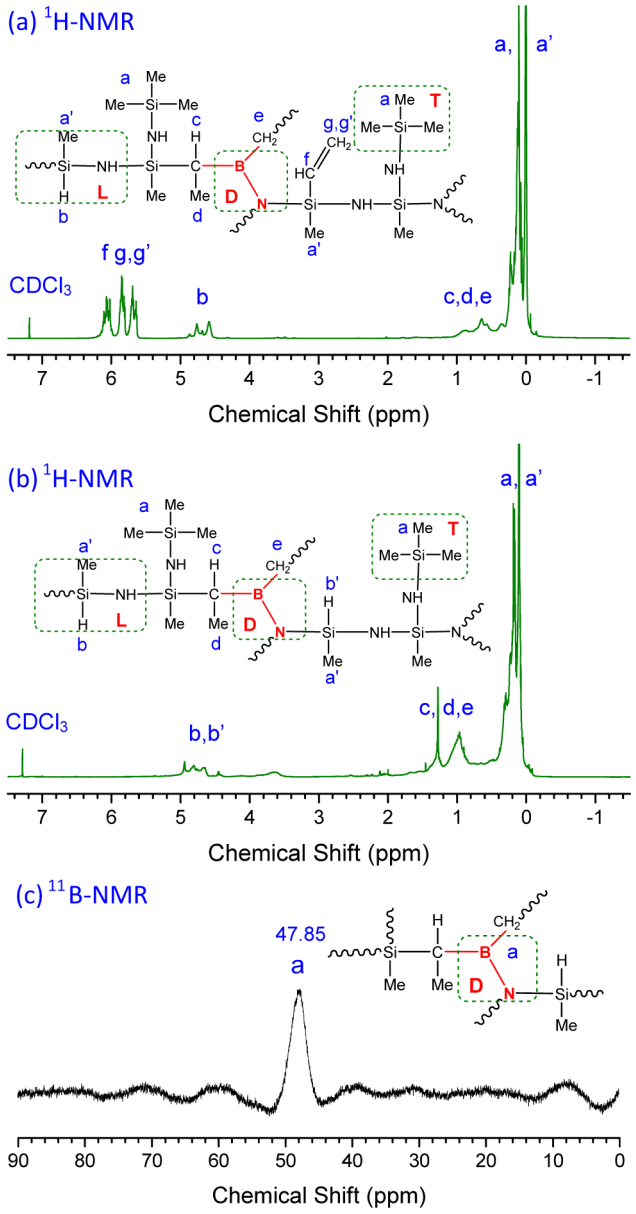

Figure 2. ^{1}H and ^{11}B NMR spectra of soluble hb-PBSZ dissolved in $CDCl_3$. (a) ^{1}H NMR spectrum of hb-PBSZ-SiH-Vi (P4), (b) ^{1}H NMR spectrum of hb-PBSZ-SiH (P1), and (c) ^{11}B NMR spectrum of hb-PBSZ-SiH (P1).

amine-borane bond. Third, the residual silicon-chloride bonds of TTMCB and DCMS were further aminolyzed at 180 °C to form the hb-PBSZ through the distillation of volatile trimethylchlorosilanes and byproducts.

As illustrated in Scheme 2, the dendritic, linear and terminal units of the hb-PBSZ are aminedialkylborons ($(—C_2H_4)_2—B—N=$), disilazane $—SiRCH_3—NH—SiRCH_3—$) and trimethylsilyl groups ($—NH—Si(CH_3)_3$), respectively. The presence of aminedialkylborons was confirmed by the characteristic signals at 47.85 ppm for P1 and 46.92 ppm for P4 in the ^{11}B NMR spectra shown in Figure 2c and Supporting Information Figure S3, respectively. Accordingly, the linear and terminal units of P1 and P4 can also be identified by ^{1}H NMR characterization, shown in Figure 2a and b. Because the dendritic, linear and terminal units are characterized via two different techniques (^{11}B NMR and ^{1}H NMR), the degree of

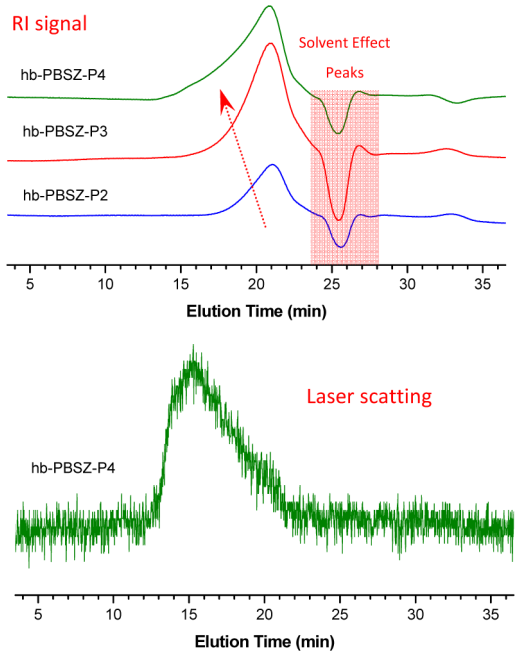

Figure 3. SEC traces (RI signal and representative laser scatting signals) of the obtained hb-PBSZ samples P2–P4 detected at a flow rate of 0.5 mL/min in THF at 25 °C.

branching or terminal index of the hb-PBSZ is difficult to measure.[47−50] However, the single main peak in the ^{11}B NMR spectrum suggests a regular hyperbranched topologic structure.

Boron is introduced into the backbone of hb-PBSZ as a result of the A_2+B_6 polymerization approach, and its content can be tuned by varying the feed ratio of TDSB and DCMS. In other words, hb-PBSZ with differing boron content can be obtained depending on the amount of TDSB employed. According to the ICP-AES data, boron is qualitatively detected in all the hb-PBSZ (P1–P4). However, the detected boron content is lower than the value calculated from the initial reactant ratio because the boron is only partially dissolved in the boiling mixture of nitric acid and hydrochloric acid during the sample treatment in preparation for the measurement.

It should be noted that some silicon chloride bonds will remain if the aminolysis reaction is not completed. These are visible in the TGA-mass spectrum. As shown in Supporting Information Figure S4, the thermolysis of P2 was accompanied by a weak evolution of hydrogen chloride (m/z = 36), caused by the dehydrochlorination of the residual silicon chloride group in the polymer. However, hydrogen chloride was not detected for the other three hb-PBSZ (P1, P3, and P4), indicating that their silicon chloride bonds have been fully aminolyzed.

Pyrolysis Behavior of Hyperbranched Polyborosilazanes. The conversions of the hb-PBSZ to ceramics were simultaneously investigated by TGA-mass spectrometry. From the TGA curves in Figure 4, all the hb-PBSZ (P1–P4) without any cross-linking treatment underwent a rapid thermolytic degradation in the temperature range of 200–800 °C, after which the TGA curve almost leveled off. The ceramic yield was 40–50% at a temperature of 1400 °C. The hb-PBSZ-SiH compounds (P1, P2) show a slightly higher ceramic yield than the hb-PBSZ-SiH-Vi compounds (P3, P4). However, after the polymers were thermally cross-linked at 400 °C for 1 h, the thermolytic degradation of the cross-linked samples only

DOI: 10.1021/am509129a
ACS Appl. Mater. Interfaces 2015, 7, 6733−6744

Table 1. Main Results of the Polymerization of Hyperbranched Polyborosilazanes[a]

sample name	monomers	feed ratio	main units	M_n	M_n	PDI
Hb-Pbsz-Sih-11 (P1)	Tsdb + Dcms	1:1.05	$(-C_2H_4)_2-B-N=$ $-SiRCH_3-NH-SiHCH_3-$ $-NH-Si(CH_3)_3$	9640	6310	1.53
Hb-Pbsz-Sih-13 (P2)	Tsdb + Dcms	1:5.08	$(-C_2H_4)_2-B-N=$ $-SiRCH_3-NH-SiHCH_3-$ $-NH-Si(CH_3)_3$	4700	2910	1.62
Hb-Pbsz-Sih-Vi-13 (P3)	Tsdb + Dcms + Dcmvs	1:2.07:1.04	$(-C_2H_4)_2-B-N=$ $-SiHCH_3-NH-SiViCH_3-$ $-NH-Si(CH_3)_3$	4570	2690	1.70
Hb-Pbsz-Sih-Vi-15 (P4)	Tsdb + Dcms + Dcmvs	1:3.49:1.66	$(-C_2H_4)_2-B-N=$ $-SiHCH_3-NH-SiViCH_3-$ $-NH-Si(CH_3)_3$	12700	7870	1.61

[a]Both the molecular weight (M_w) and the polydispersity index (PDI) were determined by triple-SEC.

Scheme 3. Proposed Reaction Mechanism for the Synthesis of the Soluble Hyperbranched Polyborosilazane hb-PSBZ-SiH

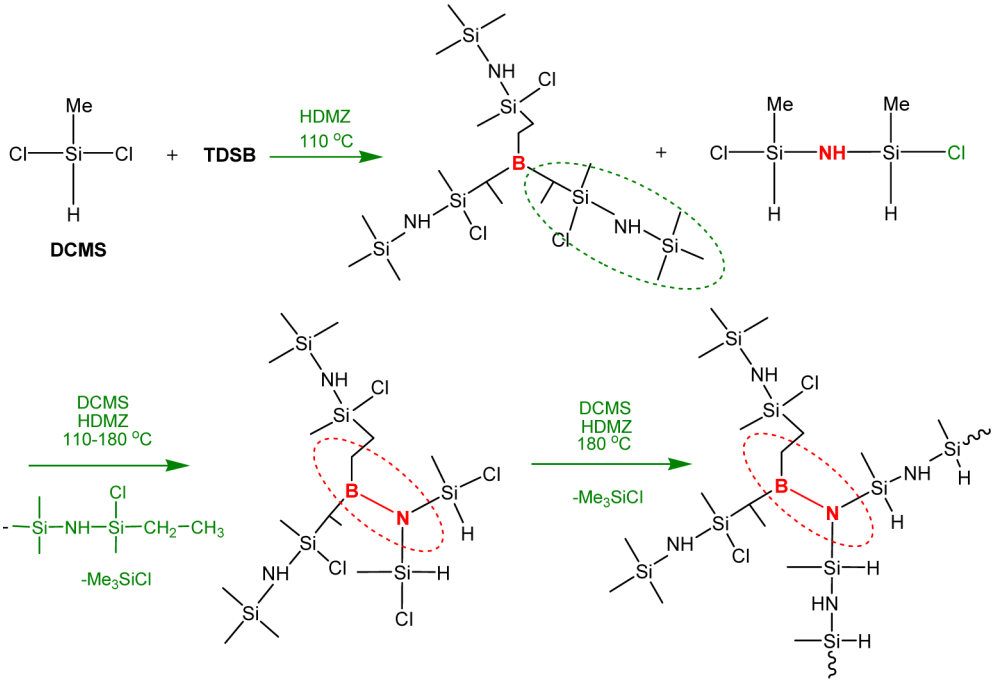

occurred in the temperature range of 420−800 °C with a yield of 75−85% at 1400 °C.

Simultaneous TGA and mass spectrometry can help to reconstruct the reactions during the pyrolysis step. As shown in Figure 5, the thermolysis of the hb-PBSZ in the temperature range of 200−800 °C was mainly accompanied by the evolution of H_2 (m/z = 2), hydrocarbons such as CH_x^+ (x = 2−3, m/z = 14−15) and CH_4 (m/z = 16), NH^+ (m/z = 15), NH_2^+ (m/z = 16), NH_3 (m/z = 17), H_2O (m/z = 18), and CO (m/z = 28), as well as a small number of oligomer fragments (m/z = 43−45). The evolution of H_2O and CO is caused by the oxidation of methyl groups, CH_4 and H_2 during pyrolysis. The H_2 evolution starting at 500 °C can be linked to the dehydrocoupling reactions of Si−H and N−H groups, while the NH_2^+, CH_4 (m/z =16) and NH^+, CH_3^+ (m/z = 15) evolution in the temperature range of 250−800 °C is from the decomposition of transamination reactions, Si-CH_3 groups and the cleavage of C−C bonds. However, there is no evolution of NH_2^+, CH_4 (m/z =16) and NH^+, CH_3^+ (m/z =15) for the cross-linked P1 in the low temperature range of 250−450 °C. This difference is also observed for P3 as shown in Supporting Information Figure S5 and accounts for the high ceramic yields after thermal cross-linking for all the hb-PBSZ.

In the case of the hb-PBSZ, several factors favor conversion from organic networks to inorganic ceramics. First, the hb-PBSZ possesses multiple Si−H, N−H, and vinyl functional groups. The hydrosilylation between Si−H/vinyl,[51] the Si−H/N-H dehydrocoupling,[52,53] the Si−H/Si-H dehydrocoupling,[54] and the polymerization of vinyl groups[55] all promote the formation of highly cross-linked networks during the heating step. Second, the boron in the backbones of the hb-PBSZ is able to increase the cross-linking density by promoting the dehydrocoupling reaction. Third, the hyperbranched structure is helpful in decreasing volatile fragments resulting from the backbone cleavage during pyrolysis.[56,57] Soluble hb-PBSZ are therefore very promising for the preparation of thermally stable SiBCN ceramics.

Pyrolyzed Ceramics from Hyperbranched Polyborosilazanes. After pyrolysis of the hb-PBSZ (P1−P4) under a protective argon atmosphere at 900 °C, bulk ceramic products

DOI: 10.1021/am509129a
ACS Appl. Mater. Interfaces 2015, 7, 6733−6744

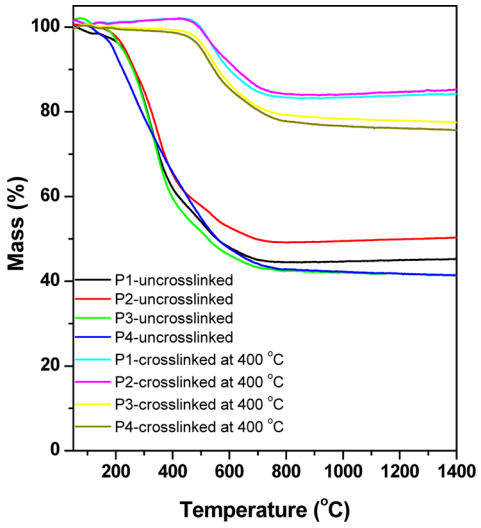

Figure 4. TGA thermograms of representative hb-PBSZ samples of the polymers P1−P4 measured at a scanning rate of 10 K/min under an argon atmosphere.

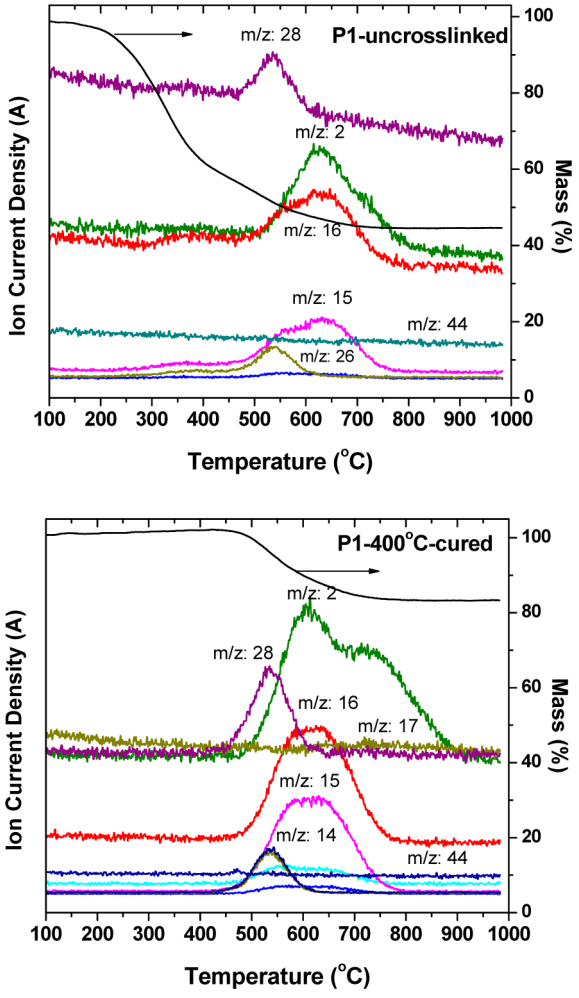

Figure 5. TGA-mass spectrum curves of representative hb-PBSZ samples of P1 measured at a scanning rate of 10 K/min under an argon atmosphere.

were formed and labeled as C1, C2, C3, and C4, respectively. XPS analysis revealed the existence of silicon, boron, carbon, nitrogen, and oxygen in the resulting ceramics. The two-dimensional element images show that boron and silicon are uniformly dispersed in the SiBCN ceramics. This analysis was performed with ICP-AES, the combustion-coulomb method and oxygen-azote mensuration equipment (sample grade = 10 g) as presented in Table 2. The atomic composition of boron is in the range of 6.0−8.5% and the formulas for C1−C4 are $Si_1B_{0.19}C_{1.21}N_{0.39}O_{0.08}$, $Si_1B_{0.30}C_{1.51}N_{0.64}O_{0.10}$, $Si_1B_{0.17}C_{1.15}N_{0.41}O_{0.07}$, and $Si_1B_{0.27}C_{1.38}N_{0.47}O_{0.09}$, respectively. It is clear that the boron content is in good agreement with the boron content of the polymers. The quaternary SiBCN ceramics from the hb-PBSZ can be compared with the $Si_{3.0}B_{1.0}C_{4.2}N_{2.4}$ ceramic obtained using the $[B(C_2H_4SiCH_3NR')_3]_n$ (C_2H_4 = $CHCH_3$ and CH_2CH_2 and R′ = −H) preceramic polymer[58] and periodic mesoporous $Si_{3.0}B_{1.0}C_{3.9}N_{1.8}$ frameworks.[59]

The existence of boron in the quaternary SiBCN ceramics was further confirmed by the B 1s XPS spectrum in Figure 6. The deconvolution of the B 1s spectrum (Figure 6e) for C1 presents three peaks centered at 187.1, 188.5, and 190.1 eV which are associated with B−B bonding, B−C bonding, and B−N bonding, respectively, suggesting that these bonds are found in the ceramics. More detailed information on the ceramic components was revealed by the XPS spectra. For the ceramics C1−C4, amorphous silicon nitrides with a Si 2p bonding energy of 101.7 eV and a N 1s bonding energy of 397.5 eV were detected along with graphitic carbon with a C 1s bonding energy of 284.7 eV. Amorphous silicon carbide was also identified by the C 1s bonding energy of 282.7 eV. In addition to the graphite-like carbon, carbon attached to oxygen via a single bond (B.E.=286 eV) was found in the ceramic C4, and carbon attached to oxygen through a single bond (B.E.=286 eV) and a double bond (B.E.=288.2 eV) was found in all ceramics C1−C4. This type of carbon is usually attributed to a carbon dioxide contamination on the sample surface that occurred prior to the XPS measurement.[60,61] Some oxygen from absorption on the ceramic powder surface prior to the measurement can also be observed. Due to the silicon oxide on the surface, there are extra peaks at 103.15 and 530.2 eV in the Si 2p spectrum, corresponding to Si−O_x and Ni−Si−O compounds, respectively.[62]

Crystallization and Phase Evolution of the Pyrolyzed Ceramics. The pyrolyzed ceramics were annealed at high temperature (1100−1600 °C) in a nitrogen atmosphere to study crystallization and phase evolution in the presence of boron. After the annealing, the silicon, carbon, boron and nitrogen presence in the ceramics was revealed by XPS (Figure 7). As confirmed by the two-dimensional element imaging and the element mapping, boron and silicon are uniformly dispersed in the SiBCN ceramics. In Figure 7e, the results of the deconvolution show that boron atoms are mostly bonded with N atoms, with the peaks centered at a binding energy of 190.2 and 191.4 eV.

The patterns obtained by powder XRD analysis are presented in Figure 8. Normally, for amorphous ternary SiCN ceramics, the transformation of an amorphous into crystalline material will usually occur at a temperature of approximately 1440 °C. The incorporation of boron into the amorphous structure by the thermolysis of boron-containing precursors is one of the most important ways to change the crystallization behavior.[63,64] The XRD patterns in Figure 8a and the TEM image in Figure 9a indicate that the quaternary SiBCN ceramics of C1−C4 obtained from the pyrolysis of P1−

DOI: 10.1021/am509129a
ACS Appl. Mater. Interfaces 2015, 7, 6733−6744

Table 2. Composition of SiBCN Ceramics Derived from Polymeric Precursors under 900 °C and an Argon Atmosphere

		atomic composition (%)					
polymer sample	ceramic	Si[a]	C[b]	N[c]	O[c]	B[a]	Si−B−C−N−O formula
P1	C1	34.80	42.07	13.49	3.00	6.60	$Si_1B_{0.19}C_{1.21}N_{0.39}O_{0.08}$
P2	C2	28.09	42.37	18.11	2.92	8.51	$Si_1B_{0.30}C_{1.51}N_{0.64}O_{0.10}$
P3	C3	35.81	41.04	14.66	2.48	6.00	$Si_1B_{0.17}C_{1.15}N_{0.41}O_{0.07}$

[a]The content of Si and B was determined by ICP-AES. [b]The content of C was determined by the combustion−coulomb method. [c]The content of N and O was analyzed by Oxygen-Azote mensuration equipment. The measurement grade was 10 g for each ceramic sample.

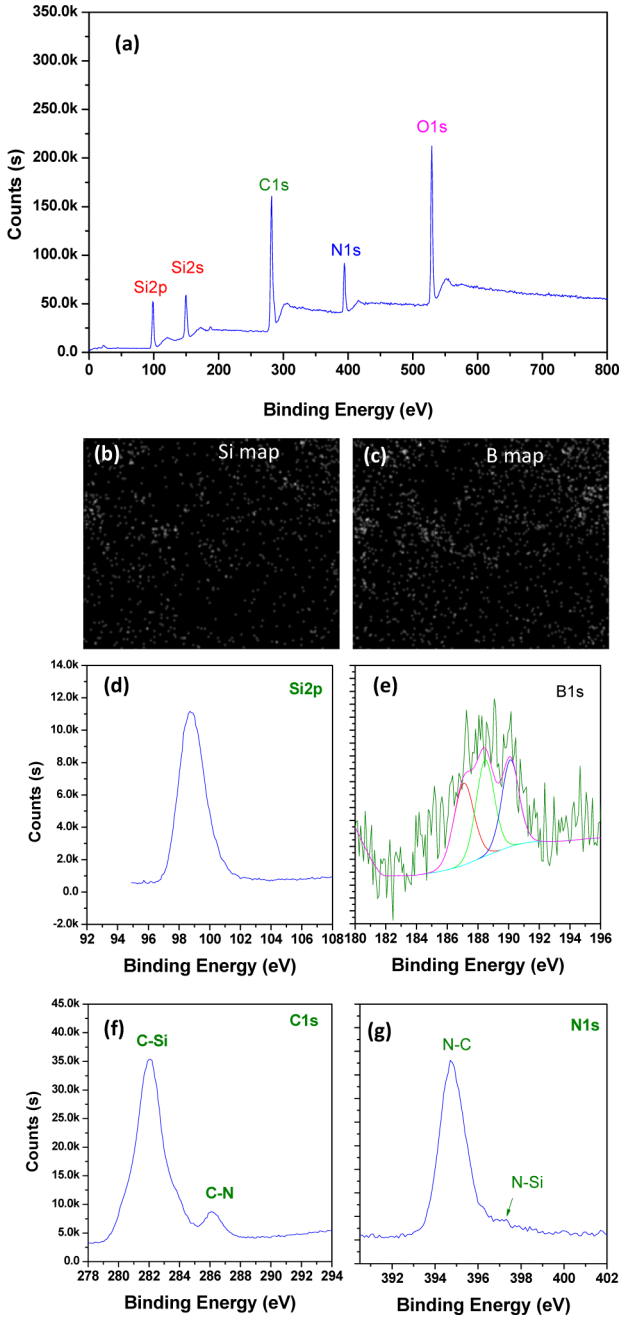

Figure 6. XPS imaging spectra for the ceramic material C1 produced from the precursor P1 and pyrolyzed at 900 °C under an argon atmosphere. (a) XPS spectrum, (b) Si map from 2D detection, (c) B map from 2D detection, (d) Si 2p spectrum, (e) B 1s spectrum, (f) C 1s spectrum, and (g) N 1s spectrum.

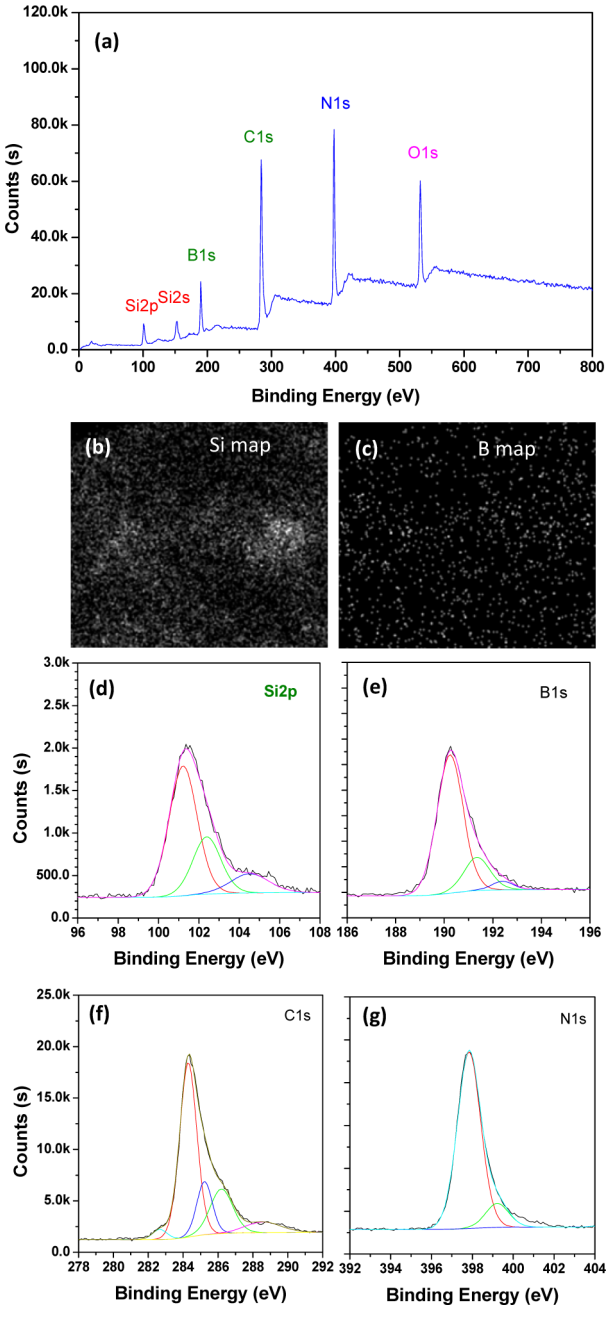

Figure 7. XPS imaging spectra for the ceramic material C1 after annealing at 1600 °C in a nitrogen atmosphere. (a) XPS spectrum, (b) Si map from 2D detection, (c) B map from 2D detection, (d) Si 2p spectrum, (e) B 1s spectrum, (f) C 1s spectrum, and (g) N 1s spectrum.

P4 at 900 °C are amorphous. When they are annealed at 1100−1500 °C, they retain their amorphous structures as confirmed by XRD (Figure 8b and c). Even when annealed at 1600 °C, only a few very broad diffraction peaks at 2θ = 37°, 60.5°, and

DOI: 10.1021/am509129a
ACS Appl. Mater. Interfaces 2015, 7, 6733−6744

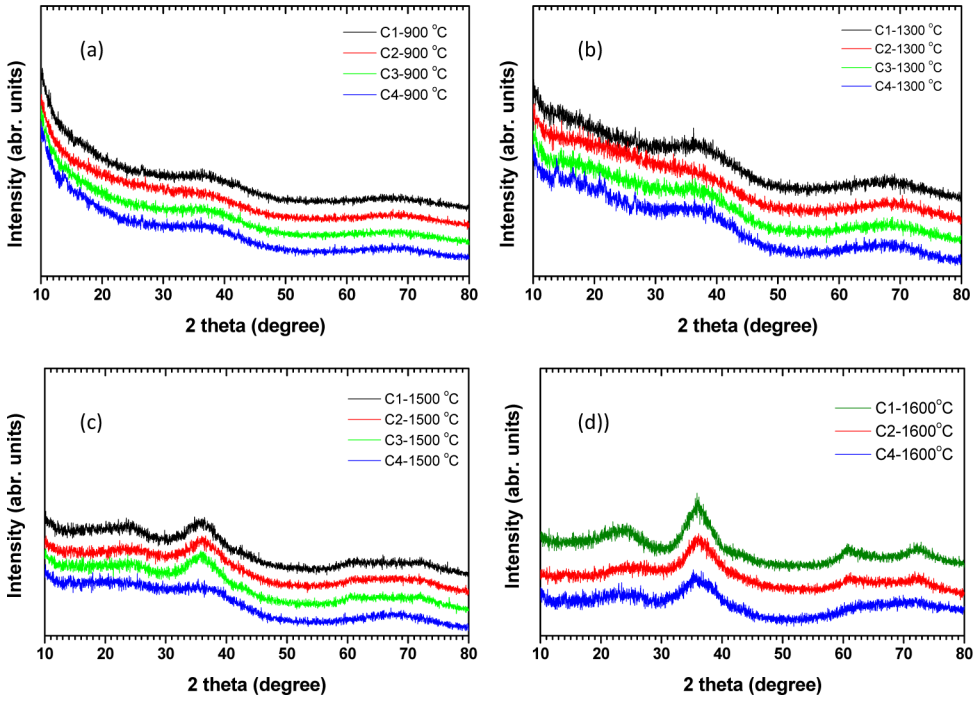

Figure 8. Powder XRD patterns of the SiBCN multiphase ceramic materials (C1−C4) pyrolyzed at 900 °C (a), annealed at 1300 (b), 1500 (c), and 1600 °C, and (d) placement in a nitrogen atmosphere for 2 h.

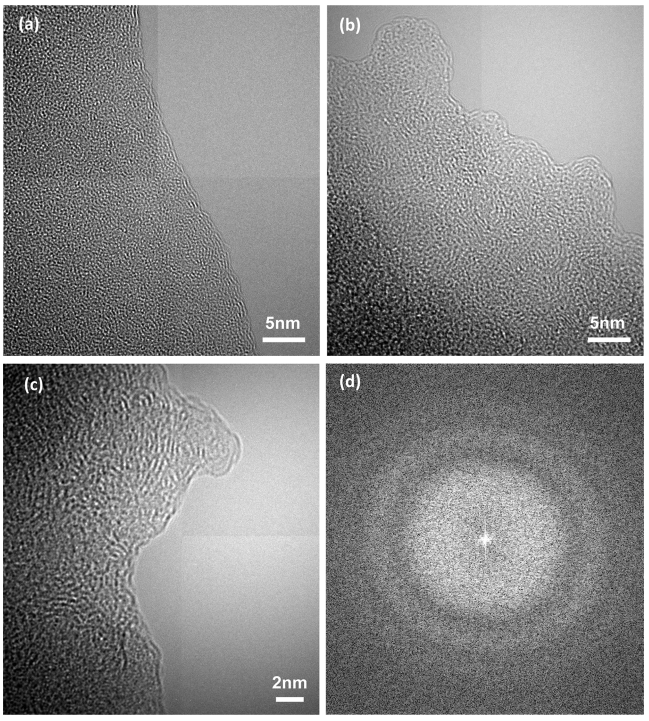

Figure 9. Representative TEM micrograph of the SiBCN multiphase ceramic material C1 pyrolyzed at 900 °C (a), annealed at 1600 °C (b), an enlarged area (c), and the corresponding fast Fourier transformed (FFT) pattern (d).

72.5° could be observed (Figure 8d), suggesting the transition of a few SiC phases from amorphous to ordered structure or small crystals. However, according to the TEM observation, there are no periodic structures, at least at the scale of 2−5 nm (Figure 9b and c). The fast Fourier transformed (FFT) pattern shown in Figure 9d, where only a few diffraction rings are visible, also demonstrates that the amorphous structure of the quaternary SiBCN ceramics can be mostly retained even when annealed at 1600 °C. For the quaternary SiBCN ceramics obtained from cross-linked polyborosilazanes via the hydroboration of polysilazanes with $H_3B{\cdot}SMe_2$, similar broad SiC diffraction peaks can be detected at 1600 °C.[65] As a comparison, for the SiBCN ceramics pyrolyzed from insoluble preceramic polymers based on boron trichloride, a partial crystallization begins at 1600 °C as indicated by tiny sharp peaks appearing at 2θ = 28°, 47°, and 56°. After 6 h of annealing at 1600 °C, the amorphous structures have been completely transformed to crystalline states,[24] while the pyrolyzed ceramics produced from hb-PBSZ maintained their amorphous state up to a high temperature, indicating that boron has a strong retarding effect on the crystallization of silicon carbonitrides.

In addition to a retarding of their crystallization, the thermal stability of SiBCN ceramics produced from hb-PBSZ was higher than that of SiCN ceramics produced from linear polysilazanes. As shown in Figure 10, the pure silicon carbonitride prepared from commercial linear polysilazane at 1100 °C (SiCN-1100 °C) decomposes at approximately 1450 °C, leading to a weight loss detected by high-temperature TGA. In this temperature range, the material decomposes into silicon carbide through the loss of nitrogen, while for the ceramic produced from P1 at 1100 °C (C1−1100 °C), the decomposition was not observed until approximately 1600 °C. For ceramics with different boron content treated at 1600 °C for 2 h (C1−1600 °C and C2−1600 °C), the thermal stability of SiBCN ceramics was maintained.

Additionally, as shown in Figure 8a, there is a smaller broad diffraction peak at approximately 25°, especially for C1 with its high boron content. This peak can most likely be attributed to graphene-like carbon structures.[66] Raman spectroscopy is an important nondestructive tool for the examination of the fine structure of free carbons, with the most prominent features of

DOI: 10.1021/am509129a
ACS Appl. Mater. Interfaces 2015, 7, 6733−6744

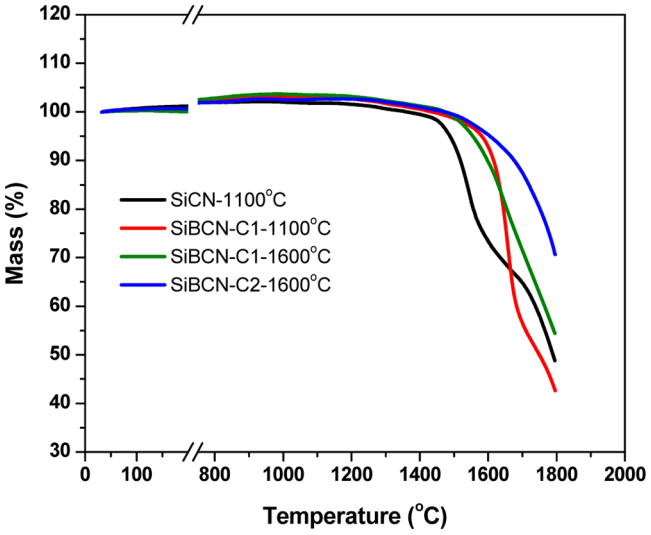

Figure 10. Results of the high-temperature thermogravimetric analysis of SiCN and SiBCN ceramics in a helium atmosphere.

free carbons being the disorder-induced D band at 1350 cm^{-1} and the G band at 1600 cm^{-1} caused by the in-plane bond stretching of sp2 carbons. The second-order *G′* band (the overtone of the D band) can always be observed in defect-free samples at 2700 cm^{-1}. Another Raman feature at 2950 cm^{-1} is associated with a D + G combination mode induced by disorder. The Gaussian−Lorentzian curve fitting of the Raman bands has been performed to extract the I_D/I_G intensity ratio.[67,68] This ratio is shown in Figure 11. After annealing, I_D/I_G value of C1 is remarkably lower than that of C4, which has lower boron content. With increasing boron content, the value of I_D/I_G apparently decreases, suggesting that the introduction of boron promotes the transition of free carbons from disordered to order states in the ceramics. Similar to the SiBCN system produced from polysilazane and $H_3B{\cdot}SMe_2$ or boron alkyl amide,[69] these intergranular ordered carbon layers also inhibited the growth of silicon carbonitride grains in SiBCN ceramics.

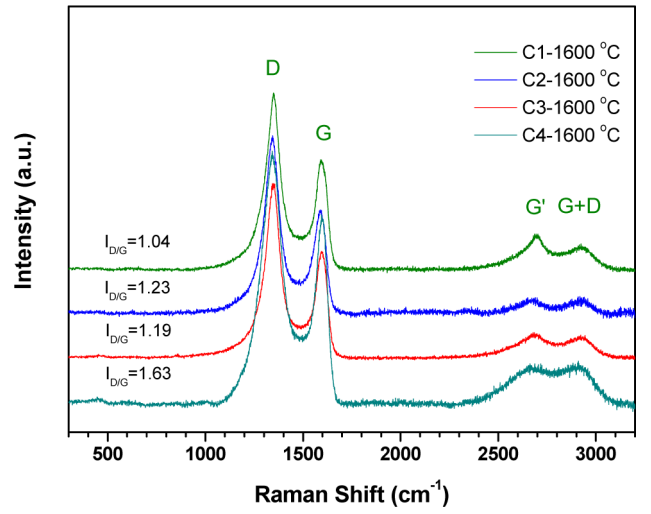

Figure 11. Raman spectra of the pyrolyzed ceramics (C1−C4) annealed at 1600 °C under a nitrogen atmosphere.

CONCLUSIONS

The convenient method to synthesize soluble hyperbranched polyborosilazanes through an aminolysis reaction between the A_2 monomers of DCMS and the B_6 monomers of tris-(dichloromethylsilylethyl)borane in the presence of HMDS was established. The dendritic units of the soluble hb-PBSZ were identified as aminedialkylborons rather than trialkylboron units. The Si−H, Si−vinyl, and Si−NH functional groups, as well as the boron in the backbones of the hb-PBSZ, enhanced ceramic yield by decreasing the elimination of volatile fragments resulting from backbone cleavage during pyrolysis. The boron in the ceramics derived from hb-PBSZ retarded the crystallization of the silicon carbonitrides and stabilized the amorphous SiBCN structures up to 1600 °C. SiBCN ceramics showed improved high temperature stability in comparison to the ternary SiCN system. In contrast to the direct aminolysis polymerization of boron-containing monomers or the hydroboration modification of polysilazane with multifunctional boranes, the A_2 + B_6 strategy developed here led to a convenient approach for synthesizing soluble hyperbranched polyborosilazanes, which provides a new perspective for the design of preceramic polymers and a huge processing advantage for making polymer-derived ceramic fibers or devices with complex structures/shapes.

ASSOCIATED CONTENT

Supporting Information

^{11}B NMR spectra, FTIR spectra, TGA-mass curves of polymers, and SEM image of SiBCN fibers. This material is available free of charge via the Internet at http://pubs.acs.org.

AUTHOR INFORMATION

Corresponding Authors

*E-mail: kongjie@nwpu.edu.cn. Tel. (fax): +86-29-88431621.
*E-mail: linan.an@ucf.edu.

Notes

The authors declare no competing financial interest.

ACKNOWLEDGMENTS

This research is supported by the Natural Science Foundation of China (21174112, 20874080 and 51372202). J.K. acknowledges the support from the Program for New Century Excellent Talents of the Education Ministry of China (NCET-11-0817).

REFERENCES

(1) Colombo, P.; Mera, G.; Riedel, R.; Soraru, G. D. Polymer-Derived Ceramics: 40 Years of Research and Innovation in Advanced Ceramics. *J. Am. Ceram. Soc.* **2010**, *93*, 1805−1837.
(2) Kroke, E.; Li, Y.-L.; Konetchny, C.; Lecomte, E.; Fasel, C.; Riedel, R. Silazane Derived Ceramics and Related Materials. *Mater. Sci. Eng., R* **2000**, *26*, 97−199.
(3) Riedel, R.; Passing, G.; Schonfelder, H.; Brook, R. J. Synthesis of Dense Silicon-Based Ceramics at Low-Temperatures. *Nature* **1992**, *355*, 714−717.
(4) Riedel, R.; Kienzle, A.; Dressler, W.; Ruwisch, L.; Bill, J.; Aldinger, F. A Silicoboron Carbonitride Ceramic Stable to 2000 Degree. *Nature* **1996**, *382*, 796−798.
(5) Sarkar, S.; Gan, Z. H.; An, L. N.; Zhai, L. Structural Evolution of Polymer-Derived Amorphous SiBCN Ceramics at High Temperature. *J. Phys. Chem. C* **2011**, *115*, 24993−25000.
(6) Wideman, T.; Cortez, E.; Remsen, E. E.; Zank, G. A.; Carrol, P. J.; Sneddon, L. G. Reactions of Monofunctional Boranes with Hydridopolysilazane: Synthesis, Characterization, and Ceramic Con-

DOI: 10.1021/am509129a
ACS Appl. Mater. Interfaces 2015, 7, 6733−6744

version Reactions of New Processible Precursors to SiNCB Ceramic Materials. *Chem. Mater.* **1997**, *9*, 2218−2230.
(7) Wang, Z.-C.; Aldinger, F.; Riedel, R. Novel Silicon−Boron−Carbon−Nitrogen Materials Thermally Stable up to 2200°C. *J. Am. Ceram. Soc.* **2001**, *84*, 2179−2183.
(8) Riedel, R.; Ruswisch, L. M.; An, L. N.; Raj, R. Amorphous Silicoboron Carbonitride Ceramic with Very High Viscosity at Temperatures above 1500°C. *J. Am. Ceram. Soc.* **1998**, *81*, 3341−3344.
(9) Ryu, H. Y.; Wang, Q.; Raj, R. Ultrahigh-Temperature Semiconductors Made from Polymer-Derived Ceramics. *J. Am. Ceram. Soc.* **2010**, *93*, 1668−1676.
(10) Zhang, L.; Wang, Y.; Wei, Y.; Xu, W.; Fang, D.; Zhai, L.; Lin, K.; An, L. N. A Silicon Carbonitride Ceramic with Anomalously High Piezoresistivity. *J. Am. Ceram. Soc.* **2008**, *91*, 1346−1349.
(11) Li, Y.; Yu, Y.; San, H.; Wang, Y.; An, L. N. Wireless Passive Polymer-Derived SiCN Ceramic Sensor with Integrated Resonator/Antenna. *Appl. Phys. Lett.* **2013**, *103*, 163505.
(12) Liu, Y.; Liew, L.; Lou, R.; An, L. N.; Bright, V.; Dunn, M.; Daily, J.; Raj, R. Application of Microforging to SiCN MEMS Fabrication. *Sens. Actuators, A* **2002**, *95*, 143−151.
(13) Hegemann, D.; Riedel, R.; Oehr, C. PACVD-Derived Thin Films in the System Si−B−C−N. *Chem. Vap. Deposition* **1999**, *5*, 61−65.
(14) Hauser, R.; Borchard, S.-N.; Riedel, R.; Ikuhara, Y. H.; Iwamoto, Y. Polymer-Derived SiBCN Ceramic and their Potential Application for High Temperature Membranes. *J. Ceramic Soc. Jpn.* **2006**, *114*, 524−528.
(15) Lu, L.; Song, Y. C.; Feng, C. X. Composition and Structure of Boron-Containing Si−N−C Fibres at High Temperature. *J. Mater. Sci. Lett.* **1998**, *17*, 599−602.
(16) Bernard, S.; Weinmann, M.; Gerstel, P.; Miele, P.; Aldinger, F. Boron-Modified Polysilazane as a Novel Single-Source Precursor for SiBCN Ceramic Fibers: Synthesis, Melt-Spinning, Curing and Cceramic Conversion. *J. Mater. Chem.* **2005**, *15*, 289−299.
(17) Puerta, A. R.; Remsen, E. E.; Bradley, M. G.; Sherwood, W.; Sneddon, L. G. Synthesis and Ceramic Conversion Reactions of 9-BBN-Modified Allylhydridopolycarbosilane: A New Single-Source Precursor to Boron-Modified Silicon Carbide. *Chem. Mater.* **2003**, *15*, 478−485.
(18) Ngoumeni-Yappi, R.; Fasel, C.; Riedel, R.; Ischenko, V.; Pippel, E.; Woltersdorf, J.; Clade, J. Tuning of the Rheological Properties and Thermal Behavior of Boron-Containing Polysiloxanes. *Chem. Mater.* **2008**, *20*, 3601−3608.
(19) Su, K.; Remsen, E. E.; Zank, G. A.; Sneddon, L. G. Synthesis, Characterization, and Ceramic Conversion Reactions of Borazine-Modified Hydridopolysilazanes: New Polymeric Precursors to Silicon Nitride Carbide Boride (SiNCB) Ceramic Composites. *Chem. Mater.* **1993**, *5*, 547−556.
(20) Wideman, T.; Su, K.; Remsen, E. E.; Zank, G. A.; Sneddon, L. G. Synthesis, Characterization, and Ceramic Conversion Reactions of Borazine/Silazane Copolymers: New Polymeric Precursors to SiNCB Ceramics. *Chem. Mater.* **1995**, *7*, 2203−2212.
(21) Brunner, A. R.; Bujalski, D. R.; Moyer, E. S.; Su, K.; Sneddon, L. G. Synthesis and Ceramic Conversion Reactions of Pinacolborane- and Diethylborazine-Modified Poly(vinylsiloxane)s. The Development of a Processable Single-Source Polymeric Precursor to Boron-Modified Silicon Carbide. *Chem. Mater.* **2000**, *12*, 2770−2780.
(22) Müller, A.; Gerstel, P.; Weinmann, M.; Bill, J.; Aldinger, F. Si−B−C−N Ceramic Precursors Derived from Dichlorodivinylsilane and Chlorotrivinylsilane. 1. Precursor Synthesis. *Chem. Mater.* **2002**, *14*, 3398−3405.
(23) Prasad, R. M.; Iwamoto, Y.; Riedel, R.; Gurlo, A. Multilayer Amorphous−Si−B−C−N/gamma-Al_2O_3/alpha-Al_2O_3 Membranes for Hydrogen Purification. *Adv. Eng. Mater.* **2010**, *12*, 522−528.
(24) Lee, J.; Butt, D. P.; Baney, R. H.; Bowers, C. R.; Tulenko, J. S. Synthesis and Pyrolysis of Novel Polysilazane to SiBCN Ceramic. *J. Non-Cryst. Solids* **2005**, *351*, 2995−3005.
(25) Nghiem, Q. D.; Jeon, J. K.; Hong, L. Y.; Kim, D. P. Polymer Derived Si−C−B−N Ceramics via Hydroboration from Borazine Derivatives and Trivinylcyclotrisilazane. *J. Organomet. Chem.* **2003**, *688*, 27−35.
(26) Jaschke, B.; Klingebiel, U.; Riedel, R.; Doslik, N.; Gadow, R. Cyclosilazanes and Borazines: Polymer Precursors to Silicon- and Boron-Containing Ceramics. *Appl. Organomet. Chem.* **2000**, *14*, 671−685.
(27) Emrick, T.; Chang, H. T.; Fréchet, J. M. J. An $A_2 + B_3$ Approach to Hyperbranched Aliphatic Polyethers Containing Chain End Epoxy Substituents. *Macromolecules* **1999**, *32*, 6380−6382.
(28) Gao, C.; Yan, D. Y. Polyaddition of B_2 and BB'_2 Type Monomers to A_2 Type Monomer. 1. Synthesis of Highly Branched Copoly(sulfone-amine)s. *Macromolecules* **2001**, *34*, 156−161.
(29) Wang, S. J.; Fan, X. D.; Kong, J.; Liu, Y.-Y. Synthesis, Characterization, and UV Curing Kinetics of Hyperbranched Polycarbosilane. *J. Appl. Polym. Sci.* **2008**, *107*, 3812−3822.
(30) Wang, S. J.; Fan, X. D.; Kong, J.; Wang, X.; Liu, Y. Y.; Zhang, G. B. A Novel Controllable Approach to Synthesize Hyperbranched Poly(siloxysilanes). *J. Polym. Sci., Part A: Polym. Chem.* **2008**, *46*, 2708−2720.
(31) Kong, J.; Schmalz, T.; Motz, G.; Müller, A. H. E. Novel Hyperbranched Ferrocene-Containing Poly(boro)carbosilanes Synthesized via a Convenient $A_2 + B_3$ Approach. *Macromolecules* **2011**, *44*, 1280−1291.
(32) Voit, B. I.; Lederer, A. Hyperbranched and Highly Branched Polymer Architectures-Synthetic Strategies and Major Characterization Aspects. *Chem. Rev.* **2009**, *109*, 5924−5973.
(33) Gao, C.; Yan, D. Hyperbranched Polymers: from Synthesis to Applications. *Prog. Polym. Sci.* **2004**, *29*, 183−275.
(34) Hong, C. Y.; You, Y. Z.; Wu, D. C.; Liu, Y.; Pan, C. Y. Thermal Control over the Topology of Cleavable Polymers: From Linear to Hyperbranched Structures. *J. Am. Chem. Soc.* **2007**, *129*, 5354−5355.
(35) Jikei, M.; Kakimoto, M. Hyperbranched Polymers: a Promising New Class of Materials. *Prog. Polym. Sci.* **2001**, *26*, 1233−1285.
(36) Li, L. W.; He, C.; He, W. D.; Wu, C. Formation Kinetics and Scaling of "Defect-Free" Hyperbranched Polystyrene Chains with Uniform Subchains Prepared from Seesaw-Type Macromonomers. *Macromolecules* **2011**, *44*, 8195−8206.
(37) Kong, J.; Schmalz, T.; Motz, G.; Müller, A. H. E. Magneto-ceramic Nanocrystals from the Bulk Pyrolysis of Novel Hyperbranched Polyferrocenyl(boro)carbosilanes. *J. Mater. Chem. C* **2013**, *1*, 1507−1514.
(38) Flory, P. J. Molecular Size Distribution in Three Dimensional Polymers. VI. Branched Polymers Containing A—R—B_{f-1} Type Units. *J. Am. Chem. Soc.* **1952**, *74*, 2718−2723.
(39) Jikei, M.; Chon, S. H.; Kakimoto, M. A.; Kawauchi, S.; Imase, T.; Watanebe, J. Synthesis of Hyperbranched Aromatic Polyamide from Aromatic Diamines and Trimesic Acid. *Macromolecules* **1999**, *32*, 2061−2064.
(40) Kricheldorf, H. R.; Fritsch, D. J.; Vakhtangishvili, L.; Schwarz, G. Multicyclic Poly(Ether Sulfone)s of Phloroglucinol Forming Branched and Cross-Linked Architectures. *Macromolecules* **2003**, *36*, 4337−4344.
(41) Unal, S.; Lin, Q.; Mourey, T. H.; Long, T. E. Tailoring the Degree of Branching: Preparation of Poly(Ether Ester)s via Copolymerization of Poly(Ethylene Glycol) Oligomers (A_2) and 1,3,5-Benzenetricarbonyl Trichloride (B_3). *Macromolecules* **2005**, *38*, 3246−3254.
(42) Müller, A.; Gerstel, P.; Weinmann, M.; Bill, J.; Aldinger, F. Correlation of Boron Content and High Temperature Stability in Si−B−C−N Ceramics. *J. Eur. Ceram. Soc.* **2000**, *20*, 2655−2659.
(43) Kong, J.; Kong, M. M.; Zhang, X. F.; An, L. N. Magnetoceramics from the Bulk Pyrolysis of Polysilazane Cross-Linked by Polyferrocenylcarbosilanes with Hyperbranched Topology. *ACS Appl. Mater. Interfaces* **2013**, *5*, 10367−10375.
(44) Ruwisch, L. M.; Duerichen, P.; Riedel, R. Synthesis of Silyl Substituted Organoboranes by Hydroboration of Vinylsilanes. *Polyhedron* **2000**, *19* (AD1−AD2), 323−330.
(45) Tseng, C.-L.; Dong, S. H. *Element−Organic Chemistry (Series 3), Chemistry of Organoboron Compounds*; Science Press: Beijing, China, 1965; Chapter 5, pp133−134.

DOI: 10.1021/am509129a
ACS Appl. Mater. Interfaces 2015, 7, 6733−6744

(46) Coates, G. E. *Organometallic Compounds*, 2nd ed; Methuen: London, 1960.
(47) Hawker, C. J.; Lee, R.; Fréchet, J. M. J. One-Step Synthesis of Hyperbranched Dendritic Polyesters. *J. Am. Chem. Soc.* **1991**, *113*, 4583−4588.
(48) Hölter, D.; Burgath, A.; Frey, H. Degree of Branching in Hyperbranched Polymers. *Acta Polym.* **1997**, *48*, 30−35.
(49) Chen, H.; Kong, J. Terminal Index: A New Way for Precise Description of Topologic Structure of Highly Branched Polymers Derived from $A_2 + B_3$ Step-wise Polymerization. *J. Phys. Chem. B* **2014**, *118*, 3441−3450.
(50) Chen, H.; Kong, J.; Tian, W.; Fan, X.-D. Intramolecular Cyclization in $A_2 + B_3$ Polymers Prepared by Step-Wise Polymerization Resulting in a Highly Branched Topology: Quantitative Determination of Cycles by Combined NMR and SEC Analytic. *Macromolecules* **2012**, *45*, 6185−6195.
(51) Choong Kwet Yive, N. S.; Corriu, R. J. P.; Leclercq, D.; Mutin, P. H.; Vioux, A. Silicon Carbonitride from Polymeric Precursors: Thermal Cross-Linking and Pyrolysis of Oligosilazane Model Compounds. *Chem. Mater.* **1992**, *4*, 141−146.
(52) Seyferth, D.; Wiseman, G. H.; Prud'homme, C. A Liquid Silazane Precursor to Silicon Nitride. *J. Am. Ceram. Soc.* **1983**, *66*, C-13−C-14.
(53) Zaheer, M.; Keenan, C. D.; Hermannsdörfer, J.; Roessler, E.; Motz, G.; Senker, J.; Kempe, R. Robust Microporous Monoliths with Integrated Catalytically Active Metal Sites Investigated by Hyperpolarized ^{129}Xe NMR. *Chem. Mater.* **2012**, *24*, 3952−3963.
(54) Ishikawa, T.; Shibuya, M.; Yamamura, T. The Conversion Process from Polydimethylsilane to Polycarbosilane in the Presence of Polyborodiphenylsiloxane. *J. Mater. Sci.* **1990**, *25*, 2809−2814.
(55) Schmidt, W. R.; Marchetti, P. S.; Interrante, L. V.; Hurley, W. J., Jr.; Lewis, R. H.; Doremus, R. H.; Maciel, G. E. Ammonia-Induced Pyrolytic Conversion of a Vinylic Polysilane to Silicon Nitride. *Chem. Mater.* **1992**, *4*, 937−947.
(56) Lücke, J.; Hacker, J.; Suttor, D.; Ziegler, G. Synthesis and Characterization of Silazane-Based Polymers as Precursors for Ceramic Matrix Composites. *Appl. Organomet. Chem.* **1997**, *11*, 181−194.
(57) McIntyre, N. S.; Zetaruk, D. G. Download Citations X-ray Photoelectron Spectroscopic Studies of Iron Oxides. *Anal. Chem.* **1977**, *49*, 1521−1529.
(58) Yan, X. B.; Gottardo, L.; Bernard, S.; Dibandjo, P.; Brioude, A.; Moutaabbid, H.; Miele, P. Ordered Mesoporous Silicoboron Carbonitride Materials via Preceramic Polymer Nanocasting. *Chem. Mater.* **2008**, *20*, 6325−6334.
(59) Majoulet, O.; Sandra, F.; Bechelany, M. C.; Bonnefont, G.; Fantozzi, G.; Joly-Pottuz, L.; Malchere, A.; Bernard, S.; Miele, P. Silicon-Boron-Carbon-Nitrogen Monoliths with High, Interconnected and Hierarchical porosity. *J. Mater. Chem. A* **2013**, *1*, 10991−11000.
(60) Huntley, D. R. The Mechanism of the Desulfurization of Benzenethiol by Nickel (110). *J. Phys. Chem.* **1992**, *96*, 4550−4558.
(61) Rufael, T. S.; Huntley, D. R.; Mullins, D. R.; Gland, J. L. Adsorption and Reaction of Dimethyl Disulfide on the Ni(111) Surface. *J. Phys. Chem. B* **1998**, *102*, 3431−3440.
(62) Finster, J.; Heeg, J.; Klinkenberg, E.-D. Chemical and Structural Order in Silicon Oxynitrides by Methods of Surface Physics. *Prog. Surf. Sci.* **1990**, *35*, 179−184.
(63) Su, K.; Remsen, E. E.; Zank, G. A.; Sneddon, L. G. Synthesis, Characterization, and Ceramic Conversion Reactions of Borazine-Modified Hydridopolysilazanes: New Polymeric Precursors to Silicon Nitride Carbide Boride (SiNCB) Ceramic Composites. *Chem. Mater.* **1993**, *5*, 547−556.
(64) Sorarù, G. D.; Pena-Alonso, R.; Kleebe, H.-J. The Effect of Annealing at 1400 °C on the Structural Evolution of Porous C-rich Silicon(boron)oxycarbide Glass. *J. Eur. Ceram. Soc.* **2012**, *32*, 1751−1757.
(65) Müller, A.; Gerstel, P.; Weinmann, M.; Bill, J.; Aldinger, F. Correlation of Boron Content and High Temperature Stability in Si−B−C−N Ceramics II. *J. Eur. Ceram. Soc.* **2001**, *21*, 2171−2177.
(66) Redlich, Ph.; Loeffler, J.; Ajayan, P. M.; Bill, J.; Aldinger, F.; Rühle, M. B−C−N Nanotubes and Boron Doping of Carbon Nanotubes. *Chem. Phys. Lett.* **1996**, *260*, 465−470.
(67) Ferrari, A. C.; Robertson, J. Interpretation of Raman Spectra of Disordered and Amorphous Carbon. *Phys. Rev. B* **2000**, *61*, 14095−14107.
(68) Ferrari, A. C.; Meyer, J. C.; Scardaci, V.; Casiraghi, C.; Lazzeri, M.; Mauri, F.; Piscanec, S.; Jiang, D.; Novoselov, K. S.; Roth, S.; Geim, A. K. Raman Spectrum of Graphene and Graphene Layers. *Phys. Rev. Lett.* **2006**, *97*, No. 18740.
(69) Jalowiecki, A.; Bill, J.; Aldinger, F. Interface Characterization of Nanosized B-Doped Si_3N_4/SiC Ceramics. *Composites, Part A* **1996**, *27*, 717−721.

DOI: 10.1021/am509129a
ACS Appl. Mater. Interfaces 2015, 7, 6733−6744